Genome-wide identification of long noncoding RNAs in CCl_4-induced liver fibrosis via RNA sequencing

ZHENGHUA GONG[1], JIALIN TANG[2], TIANXIN XIANG[3], JIAYU LIN[4], CHAOWEN DENG[5], YANZHONG PENG[5], JIE ZHENG[6] and GUOXIN HU[5]

[1]Department of Ultrasound, Peking University Shenzhen Hospital, Shenzhen PKU-HKUST Medical Center, Shenzhen, Guangdong 518036; [2]Department of Public Health, Center for Disease Control and Prevention in Jiangxi, Nanchang, Jiangxi 330029; [3]Department of Infectious Diseases, The First Affiliated Hospital of Nanchang University, Nanchang, Jiangxi 330006; [4]Department of Digestive Diseases, The Eighth Affiliated Hospital of Sun Yat-sen University, Shenzhen, Guangdong 518033; Departments of [5]Infectious Diseases and [6]Traditional Chinese Medicine, Peking University Shenzhen Hospital, Shenzhen PKU-HKUST Medical Center, Shenzhen, Guangdong 518036, P.R. China

Received March 21, 2017; Accepted April 5, 2018

DOI: 10.3892/mmr.2018.8986

Abstract. Liver fibrosis occurs as a result of chronic liver lesions, which may subsequently develop into liver cirrhosis and hepatocellular carcinoma. The involvement of long noncoding RNAs (lncRNAs) in liver fibrosis is being increasingly recognized. However, the exact mechanisms and functions of the majority of lncRNAs are poorly characterized. In the present study, the hepatotoxic substance carbon tetrachloride (CCl_4) was employed to induce liver fibrosis in an animal model and agenome-wide identification of lncRNAs in fibrotic liver tissues compared with CCl_4 untreated liver tissues was performed using RNA sequencing. Sprague-Dawley rats were treated with CCl_4 for 8 weeks. Histopathogical alterations were observed in liver tissues, and serum levels of alanine aminotransferase, aspartate aminotransferase, transforming growth factor-β1 and tumor necrosis factor-α were significantly higher, in the CCl_4-treated group compared with the CCl_4 untreated group. RNA sequencing of liver tissues demonstrated that 231 lncRNAs and 1,036 mRNAs were differentially expressed between the two groups. Furthermore, bioinformatics analysis demonstrated that the differentially expressed mRNAs were predominantly enriched in 'ECM-receptor interaction', 'PI3K-Akt signaling pathway' and 'focal adhesion' pathways, all of which are essential for liver fibrosis development. Validation of 12 significantly aberrant lncRNAs by reverse transcription-quantitative polymerase chain reaction indicated that the expression patterns of 11 lncRNAs were consistent with the sequencing data. Furthermore, overexpression of lncRNA NR_002155.1, which was markedly downregulated in CCl_4-treated liver tissues, was demonstrated to inhibit HSC-T6 cell proliferation *in vitro*. In conclusion, the present study determined the expression patterns of mRNAs and lncRNAs in fibrotic liver tissue induced by CCl_4. The identified differentially expressed lncRNAs may serve as novel diagnostic biomarkers and therapeutic targets for liver fibrosis.

Correspondence to: Professor Guoxin Hu, Department of Infectious Diseases, Peking University Shenzhen Hospital, Shenzhen PKU-HKUST Medical Center, 1120 Lianhua Road, Shenzhen, Guangdong 518036, P.R. China
E-mail: huguoxin8228@126.com

Professor Jie Zheng, Department of Traditional Chinese Medicine, Peking University Shenzhen Hospital, Shenzhen PKU-HKUST Medical Center, 1120 Lianhua Road, Shenzhen, Guangdong 518036, P.R. China
E-mail: zhengjie6363@sina.com

Abbreviations: lncRNAs, long noncoding RNAs; CCl_4, carbon tetrachloride; Alt, alanine aminotransferase; Ast, aspartate aminotransferase; ECM, extracellular matrix; GO, Gene Ontology; KEGG, Kyoto Encyclopedia of Genes and Genomes; RT-qPCR, reverse transcription-quantitative polymerase chain reaction; HSCs, hepatic stellate cells; H&E, hematoxylin and eosin; CCK-8, Cell Counting Kit-8

Key words: long noncoding RNA, RNA sequencing, liver fibrosis, carbon tetrachloride, bioinformatics analysis

Introduction

Liver fibrosis, characterized by excessive deposition of extracellular matrix (ECM) and distortion of the normal liver architecture, occurs as a result of liver injuries, such as those induced by chronic hepatitis virus, ethanol, toxic reagents or drugs (1). Liver fibrosis, considered to be a serious global health problem, may eventually develop into liver cirrhosis and, in certain cases, liver cancer, and is thus associated with high morbidity and mortality (2). Toxic reagents, predominantly the metabolic products of toxicants, reactive oxygen species, inflammatory cytokines and damage to DNA repair mechanisms, are among the common risk factors for the development of liver injury and fibrosis (3). Carbon tetrachloride (CCl_4) is widely known for its toxic effects, resulting in liver injury and liver fibrosis. Furthermore, CCl_4 has been extensively used

in studies concerning liver fibrosis (4). However, the exact molecular mechanisms underlying the toxic effects of CCl_4 have not yet been determined.

Long noncoding RNAs (lncRNAs) are commonly defined as RNA molecules with a length >200 nucleotides with limited or no protein-coding capacity (5). Increasing evidence has revealed that lncRNAs are involved in numerous biological processes, including cell proliferation, apoptosis, cell cycle, cell differentiation (6-8), nervous system development (9) and cancer metastasis (10). Furthermore, lncRNAs affect gene expression via the regulation of transcriptional, post-transcriptional and/or epigenetic mechanisms (11,12). Numerous studies have indicated the involvement of several lncRNAs in liver fibrosis, including Alu-mediated CDKN1A/p21 transcriptional regulator (13), metastasis-associated lung adenocarcinoma transcript 1 (14), maternally expressed 3 (15) and growth arrest-specific 5 (16). Despite these previous findings, other lncRNAs involved in the occurrence and development of liver fibrosis require identification.

High-throughput genome screening provides a comprehensive picture of gene expression under pathological conditions and may contribute novel insights into the mechanisms underlying liver fibrosis. Rapid developments in systems biology and bioinformatics means that the biological process and disease complexity on a systems level can be elucidated (17).

Therefore, in order to determine potential regulatory lncRNAs and investigate the expression pattern of lncRNAs with regards to the occurrence and development of liver fibrosis, the present study aimed to profile differentially expressed lncRNAs and mRNAs in CCl_4-induced liver fibrotic tissue via RNA sequencing. Bioinformatics analyses, including Gene Ontology (GO) and Kyoto Encyclopedia of Genes and Genomes (KEGG) pathway analysis, were performed to improve the classification of differentially expressed mRNAs between the CCl_4-treated and CCl_4 untreated liver tissues. In order to validate the RNA sequencing data, reverse transcription-quantitative polymerase chain reaction (RT-qPCR) was performed and a significantly differentially expressed lncRNA, NR_002155.1, was identified, which, to the best of our knowledge, has not been previously investigated. The present study aimed to elucidate further candidate diagnostic biomarkers and treatment targets for liver fibrosis.

Materials and methods

Rat liver fibrosis induced by CCl_4. Male Sprague-Dawley rats (n=20; 8 weeks old) weighing 200-220 g were obtained from Guangdong Medical Laboratory Animal Center (Guangzhou, China). The rats were housed in polycarbonate cages under standard laboratory conditions at a temperature of 22˚C, a relative humidity of 55% and 12 h light/dark cycle. Rats were fed with standard laboratory food pellets and water *ad libitum*. Rats were housed in these conditions for 7 days prior to CCl_4 administration. CCl_4 was purchased from Tianjin Fuyu Fine Chemical Co., Ltd. (Tianjin, China). Rats were equally divided into two groups by random sampling: Untreated group and CCl_4-treated group. Rats in the CCl_4-treated group were injected intraperitoneally with a 0.6 mg/kg mixture of CCl_4 and corn oil [1:1 (v/v)] twice a week for 8 weeks. Rats in the control group were treated with equal volumes of corn oil. The body weight and clinical symptoms of the rats were observed twice a week until the termination of the experiment. Blood and liver tissues were collected from each rat. Blood was collected for serum biochemistry and cytokine investigation. Liver tissues were sliced into sections and preserved in 4% paraformaldehyde for 48 h at room temperature or TRIzol reagent at 4˚C (Invitrogen; Thermo Fisher Scientific, Inc., Waltham, MA, USA) for histological staining and RNA extraction, respectively. The liver tissues of three rats from each group were frozen in liquid nitrogen in preparation for RNA sequencing. The animal experimental procedures in the present study were performed in accordance with the Guide for Animal Care (18) and Use and were approved by the Animal Ethics Committee of Peking University Shenzhen Hospital (Shenzhen, China).

Cell culture and overexpression of NR_002155.1 in HSC-T6 cells. The HSC-T6 rat hepatic stellate cell (HSC) cell line was purchased from the Institute of Cell Research, Chinese Academic of Sciences (Shanghai, China). The HSC-T6 cells were cultured in Dulbecco's modified Eagle's medium (DMEM; Gibco; Thermo Fisher Scientific, Inc.) supplemented with 10% fetal bovine serum (FBS; Gibco; Thermo Fisher Scientific, Inc.), 100 μg/ml streptomycin and 100 U/ml penicillin. They were incubated at 37˚C with an atmosphere of 5% CO_2.

Ad-NR_002155.1 was purchased from Vigene Biosciences, Inc. (Rockville, MD, USA). The NR_002155.1 sequence (https://www.ncbi.nlm.nih.gov/nuccore/NR_002155.1?report=fasta) or nonsense sequence (negative control; ATGCCAACCACGGCGCCGCCCACA GCACTCCTGCTGCTGGCGGCCGCCCTTTAACCGACA AGGACCTGCGCGGGTGAGTGCCGGGTCCGGAGG GAAATGGCCTCTGAATTAGGGGCGAATTAGGCA CCTGGGAAAAAAGGTCTCCACGTCGCACACCAG ACCCTGCTCCTTCTCCACCGGCGTCCAGAACCCCGC GCCCTGCTCCCTGCCCGGCCCGCGCTTGGGCCC GGGAAAACGGGAGGAGATCAGGGTTTCACGCGC ACCGCCCCCAGGCTCACACTCGGTTCGGTATTTCGT CACCGCGGTGTCCCGGCCCGGCCTCGGTTCACCACG GTTCATCTCTGTCG) was subcloned into the adenovirus shuttle plasmid vector pAd-EF1a-GFP (Vigene Biosciences, Inc.). Homologous recombination was used with regards to the pBHGlox_E1, 3 Cre and shuttle plasmids in order to generate Ad-NR_002155.1. HSC-T6 cells were subsequently infected with Ad-NR_002155.1. Cells ($1x10^5$) were seeded in 6 well plates. After 12 h, cells were infected by Ad-NR_002155.1 (multiplicity of infection=60) for 12 h. Cells were subsequently cultured in normal DMEM with 10% FBS for 48 h prior to seeding for CCK-8 and RT-qPCR assays. All cell incubations were at 37˚C with 5% CO_2.

Detection of alanine aminotransferase (Alt), aspartate transaminase (Ast), tumor necrosis factor-α (Tnf-α) and transforming growth factor-β1 (Tgf-β1) expression. Serum was obtained from whole blood by centrifugation at 12,000 x g for 15 min at 4˚C. Alt (cat ml037336), Ast (cat. no. ml12021), Tnf-α (cat. no. ml002859) and Tgf-β1 (cat. no. ml002856) in serum were detected by enzyme

Table I. Rat primer sequences for reverse transcription-quantitative polymerase chain reaction.

Transcript	Forward primer	Reverse primer
NR_002155.1	5'-gatgacccggagcaagtg-3'	5'-ctccaggtaggccctctttc-3'
XR_596496.1	5'-aaggaagaactcccatattgcat-3'	5'-acgtcagggcagaaaatgtc-3'
XR_353556.2	5'-ggtgactgacaaagaagagaagc-3'	5'-ccaggcacaaggtcaacag-3'
RGD1559724	5'-ggaaaccccgttgttttctt-3'	5'-tggttaacgtccaggcatc-3'
XR_353723.1	5'-tgtggcttctccagaccag-3'	5'-tcctgtccttcgttgatgttc-3'
XR_597361.1	5'-gcagagagctgtgtctgaacc-3'	5'-gcaaatggctgccctaga-3'
XR_591985.1	5'-tactctctcctcggatggct-3'	5'-gctttctatgtggcctggttc-3'
XR_591987.1	5'-cactggagcgtcaatcaaag-3'	5'-acttagccccacctccaagta-3'
XR_352490.2	5'-caactaagctggacccttgg-3'	5'-ggggcctcagtcttgtgag-3'
XR_361902.2	5'-tggcgtcagtgaacaacttc-3'	5'-acccgggccaaggtatag-3'
Acp1-ps1	5'-tgagagaggagaacctggatg-3'	5'-gagtcactgtacagcccagga-3'
XR_350045.1	5'-acatagatcaaaccccgagaag-3'	5'-tacagccagatgctcccagt-3'
GAPDH	5'-gacggcaagttcaacggcacagt-3'	5'-agcggaaggggcggagatgat-3'

linked-immunsorbent assay kits purchased from Shanghai Enzyme-linked Biotechnology Co., Ltd. (Shanghai, China) according to the manufacturer's protocols. The experiments were performed in triplicate.

Histological staining. The liver tissue samples from the rats were fixed in 4% paraformaldehyde at 4˚C overnight, embedded in paraffin and cut into 4 mm sections. The sections were deparaffinized in xylene and rehydrated in a graded alcohol series (100% ethanol for 5 min, 80% ethanol for 5 min; both at room temperature). The sectioned tissues were stained by Hematoxylin and eosin (H&E) staining. In brief, tissues were incubated with hematoxylin solution for 5 min and eosin solution for 1 min at room temperature. Masson staining was performed according to the manufacturer's protocols (Nanjing SenBeiJia Biological Technology Co., Ltd., Nanjing, China). Briefly, the sectioned tissues were stained with Celestine blue dye for 2 min, Mayer's hematoxylin for 2 min, followed by Ponceau S and acid fuchsin staining for 10 min, all at room temperature. The sections were photographed with a light microscope at a magnification of x100 or x200.

RNA extraction and RT-qPCR. Total RNA from tissues or cells was isolated using TRIzol reagent. The purity and concentration of RNA were quantified using the NanoDrop 2000 spectrophotometer (Thermo Fisher Scientific, Inc.). High quality isolated RNA with an optical density (OD) value 260/280>1.90 was determined as the cut-off value for RNA sequencing and RT-qPCR. Total RNA was reverse transcribed using a PrimeScript™ RT reagent Kit with gDNA Eraser (Takara Bio, Inc., Otsu, Japan), according to the manufacturer's protocol. Gene expression levels were determined via qPCR using the SYBR Premix Ex Taq™ II kit (Takara Bio, Inc.) in an ABI PRISM 7500 system (Thermo Fisher Scientific, Inc.). According to the manufacturer's protocol, the thermocycling conditions were 95˚C for 5 min, 40 cycles at 95˚C for 15 sec, 56˚C for 30 sec and 72˚C for 15 sec, followed by a final extension at 72˚C for 7 min. The housekeeping gene GAPDH was used for normalization and all experiments were performed in triplicate. The relative fold-change of the lncRNAs was calculated using the $2^{-\Delta\Delta Cq}$ method (19). The primer sequences used in the present study are listed in Table I.

RNA sequencing. Total RNA isolated from the liver tissues of three rats from each group were selected for RNA sequencing. In order to perform high-throughput sequencing, ribosomal RNA (rRNA) was depleted from total RNA by using the Ribo-Zero rRNA Removal kit (Epicentre; Illumina, Inc., San Diego, CA, USA) in accordance with the manufacturer's protocol. cDNA libraries were subsequently generated using a ScriptSeq v2 RNA-Seq Library Preparation kit (Epicentre; Illumina, Inc.) and were sequenced on an Illumina HiSeq 3000 with 101 bp paired-end reads at Guangzhou RiboBio Co., Ltd. (Guangzhou, China). The raw reads were first filtered to remove the adapter sequences and the low quality sequences were removed by the FASTX-Toolkit v0.0.13 (hannonlab.cshl.edu/fastx_toolkit/index.html.). The subsequent clean reads were mapped to the reference genome Rnor_6.0 (asia.ensembl.org/Rattus_norvegicus/Info/Index) with TopHat v2.0.13 (20). The number of reads mapped to each gene was determined using gfold v1.1.2 (21). Differential expression was assessed using Cufflinks (22) with fragments/kb of transcript per million fragments mapped and read counts as the input. Differentially expressed genes were identified according to the following criteria: Fold-change >2 and adjusted P-value <0.001.

GO and KEGG pathway analysis. Differentially expressed mRNAs in fibrotic liver tissues were determined via GO analysis and KEGG pathway analysis. With regards to GO analysis (http://geneontology.org/), the aberrantly expressed mRNAs were classified into three items by enrichment analysis: Biological process, cellular component and molecular function. KEGG pathway analysis (www.genome.jp/kegg/) was performed in order to analyze the potential pathways enriched by the differentially expressed mRNAs.

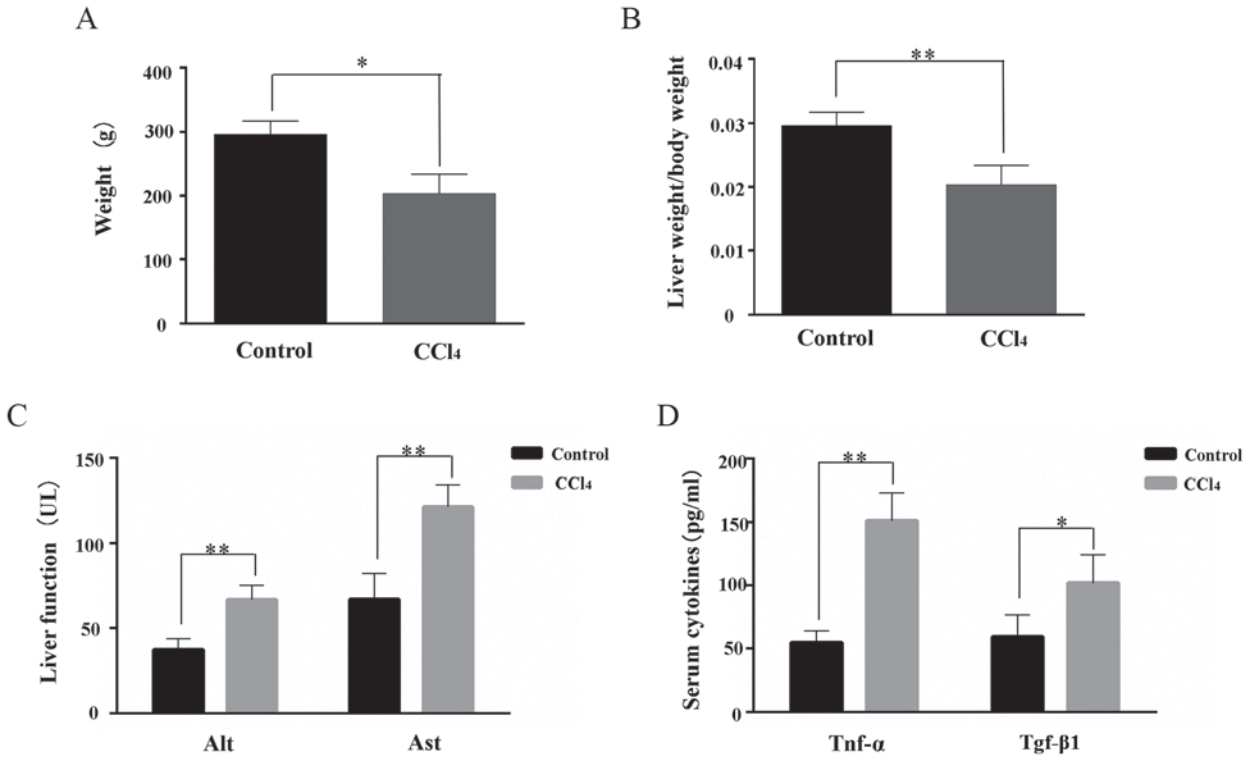

Figure 1. Body weight, liver/body weight ratio and the serum levels of Alt, Ast, Tnf-α and Tgf-β1 in rats treated with or without CCl_4. (A) Body weight and (B) liver/body weight ratio were determined after 8 weeks of CCl_4 treatment. Serum levels of (C) Alt and Ast and (D) Tnf-α and Tgf-β1 were determined using commercial kits. *P<0.05 and **P<0.01, as indicated. Alt, alanine aminotransferase; Ast, aspartate aminotransferase; Tnf-α, tumor necrosis factor-α; Tgf-β1, transforming growth factor-β1; CCl_4, carbon tetrachloride.

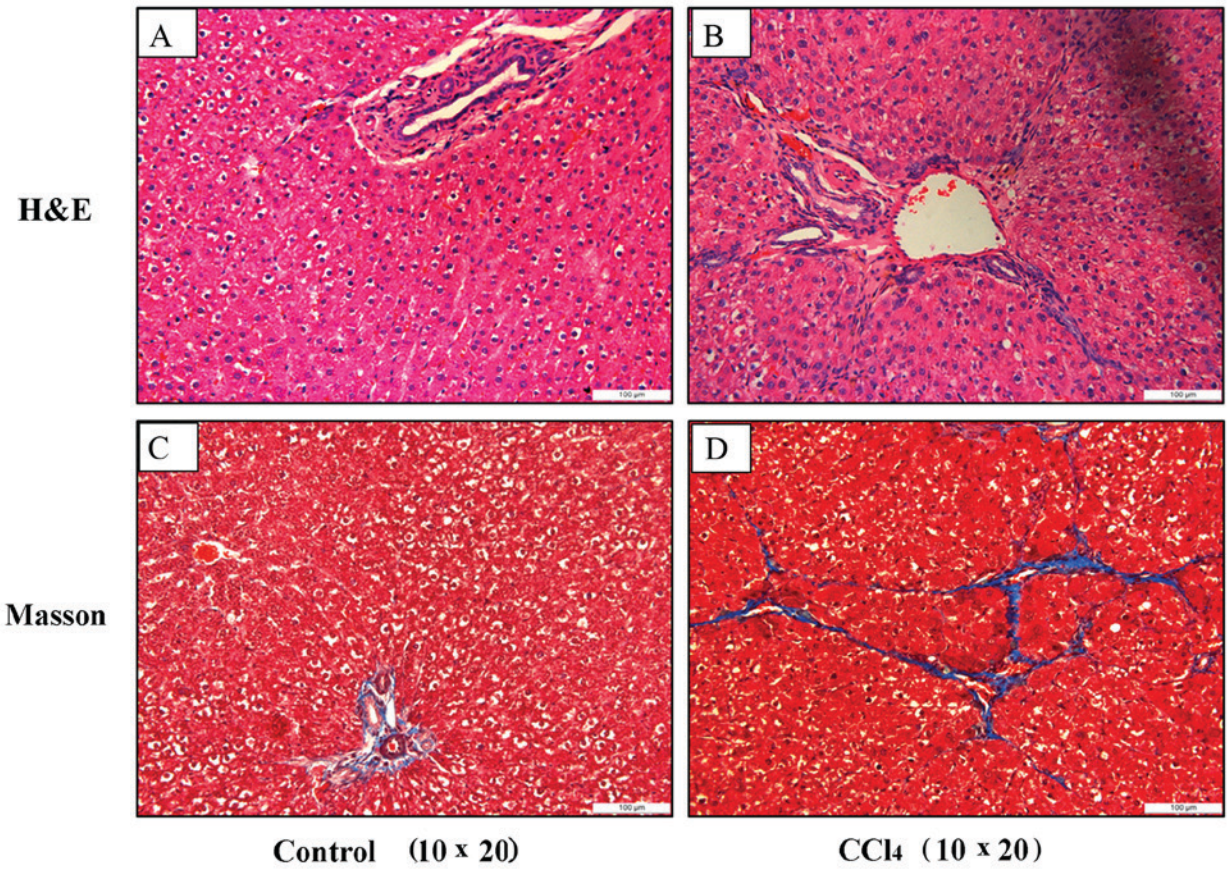

Figure 2. Histological staining in liver tissues of untreated and CCl_4-treated rats. H&E staining was performed on liver tissues from (A) untreated and (B) CCl_4-treated rats (magnification, x200). Masson staining was performed on liver tissues from (C) untreated and (D) CCl_4-treated rats (magnification, x200). Scale bar, 100 μM. CCl_4, carbon tetrachloride; H&E, hematoxylin and eosin.

Cell Counting Kit-8 (CCK-8) assay. A CCK-8 assay (Dojindo Molecular Technologies, Inc., Kumamoto, Japan) was used to perform the cell proliferation assay. The transfected HSC-T6 cells were plated in 96-well plates at a density of 1,000 cells/well. Following incubation at 37˚C for 12, 24, 48 and 72 h time intervals, the OD values of absorbance were determined using a microplate reader (Bio-Rad Laboratories, Inc., Hercules, CA, USA) at a wavelength of 450 nm, in accordance with the manufacturer's protocol. All experiments were performed in triplicate.

Statistical analysis. Data from at least three independent experiments were presented as the mean ± standard deviation. Student's t-tests were used to analyze the statistical significance of RT-qPCR, Alt, Ast, Tnf-α, Tgf-β1 and cell proliferation analyses. Multiple comparisons of the expression of NR_002155.1 among the three HSC-T6 cell groups were performed using one-way analysis of variance followed by the Student-Newman-Keuls post-hoc test. $P<0.05$ was considered to indicate a statistically significant difference. SPSS v19.0 software (IBM Corp., Armonk, NY, USA) was used to analyze the data.

Results

Liver injury and fibrosis induction. At the termination of the experiment, the body weight and the liver/body weight ratio were significantly reduced in the CCl_4-treated rats compared with the untreated group (Fig. 1A and B).

Liver functions, measured by Alt and Ast levels in the serum, were also investigated. The results demonstrated that Alt and Ast expression levels were significantly increased in the CCl_4-treated group compared with the untreated group (Fig. 1C). Alterations in the serum levels of Tnf-α and Tgf-β1 are presented in Fig. 1D. The expression levels of Tnf-α and Tgf-β1 were significantly increased in the CCl_4-treated rats, indicating an increased inflammatory response in the CCl_4-treated rats following treatment.

As demonstrated in Fig. 2A and B, H&E staining indicated that treatment with CCl_4 markedly increased levels of inflammation and cell infiltration surrounding the liver cells, and also resulted in an unclear hepatic lobular structure compared with that of the untreated group. The results of the Masson staining indicated that paraplastic connective tissues destroyed the structure of the liver lobule and that marked levels of fibrosis developed in the liver tissue of the CCl_4-treated group, compared with the untreated group where no marked liver fibrosis development was observed (Fig. 2C and D).

Differentially expressed lncRNAs and mRNAs. A total of 16,113 lncRNAs and 35,362 mRNAs were identified by RNA sequencing. Compared with the untreated group, the CCl_4-treated group had 231 differentially expressed lncRNAs (fold-change >2), which included 102 upregulated and 129 downregulated lncRNAs. The top 10 upregulated and top 10 downregulated lncRNAs with the largest fold-change are presented in Table II. Expression profiling data demonstrated that 1,306 mRNAs, consisting of 1,028 upregulated and 278 downregulated mRNAs, were differentially expressed between the two groups.

Table II. Top 10 upregulated and downregulated lncRNAs between untreated and carbon tetrachloride-treated liver samples.

A, Upregulated lncRNAs

Sequence name	Fold-change	P-value
LOC100364116	83.55	1.19×10^{-24}
NR_002155.1	36.61	1.29×10^{-10}
XR_595047.1	23.47	9.10×10^{-7}
LOC103692060	23.47	9.10×10^{-7}
XR_595045.1	23.47	9.10×10^{-7}
XR_595048.1	22.53	1.70×10^{-6}
XR_595044.1	22.53	1.70×10^{-6}
XR_595046.1	21.59	3.18×10^{-6}
XR_595680.1	19.71	2.11×10^{-10}
XR_355421.2	18.77	2.05×10^{-5}

B, Downregulated lncRNAs

Sequence name	Fold-change	P-value
XR_594950.1	36.57	1.31×10^{-271}
XR_592258.1	32.31	7.51×10^{-163}
XR_591976.1	21.31	6.12×10^{-11}
LOC102554180	17.04	8.63×10^{-5}
XR_358112.2	12.25	5.14×10^{-6}
XR_356224.1	11.72	9.83×10^{-6}
XR_596548.1	10.65	3.56×10^{-5}
XR_350587.2	9.94	1.11×10^{-6}
NR_027324.1	9.87	1.63×10^{-120}
XR_352538.2	8.43	6.66×10^{-16}

lncRNAs, long noncoding RNAs.

Bioinformatics analysis of differentially expressed mRNAs. In order to identify the potential function of dysregulated mRNAs in fibrotic rat liver tissues compared with normal liver tissues, GO analysis was performed, during which three items were described (biological process, cellular component and molecular function). Differentially expressed mRNAs were predominantly enriched in the following GO terms: 'Muscle system process', 'biological adhesion' and 'cell adhesion' for biological process terms; 'proteinaceous extracellular matrix', 'extracellular matrix' and 'myofibril' for the cellular component terms; and 'extracellular matrix structural region', 'cytoskeletal protein binding' and 'calcium ion binding' for molecular function terms. The top 10 enriched GO terms for biological process, cellular component and molecular function are presented in Fig. 3.

In addition, pathway analysis was performed with reference to the KEGG database and 27 pathways presenting significant differences ($P<0.05$) in gene expression were identified between the CCl_4-treated and untreated rat liver tissues (data not shown). As revealed in Fig. 4, the differentially expressed

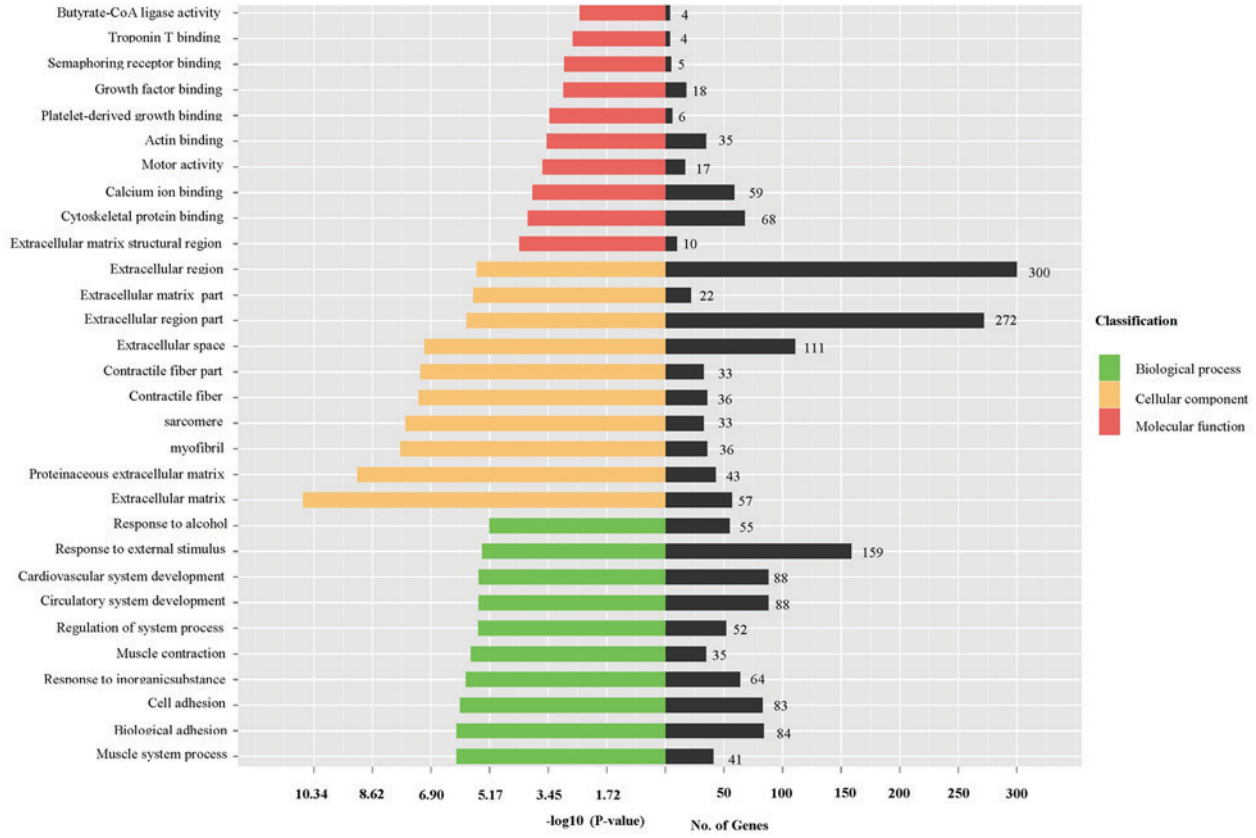

Figure 3. GO analysis of differentially expressed mRNAs in liver fibrosis. Top 10 enriched GO terms of biological process, cellular component and molecular function. GO, Gene Ontology.

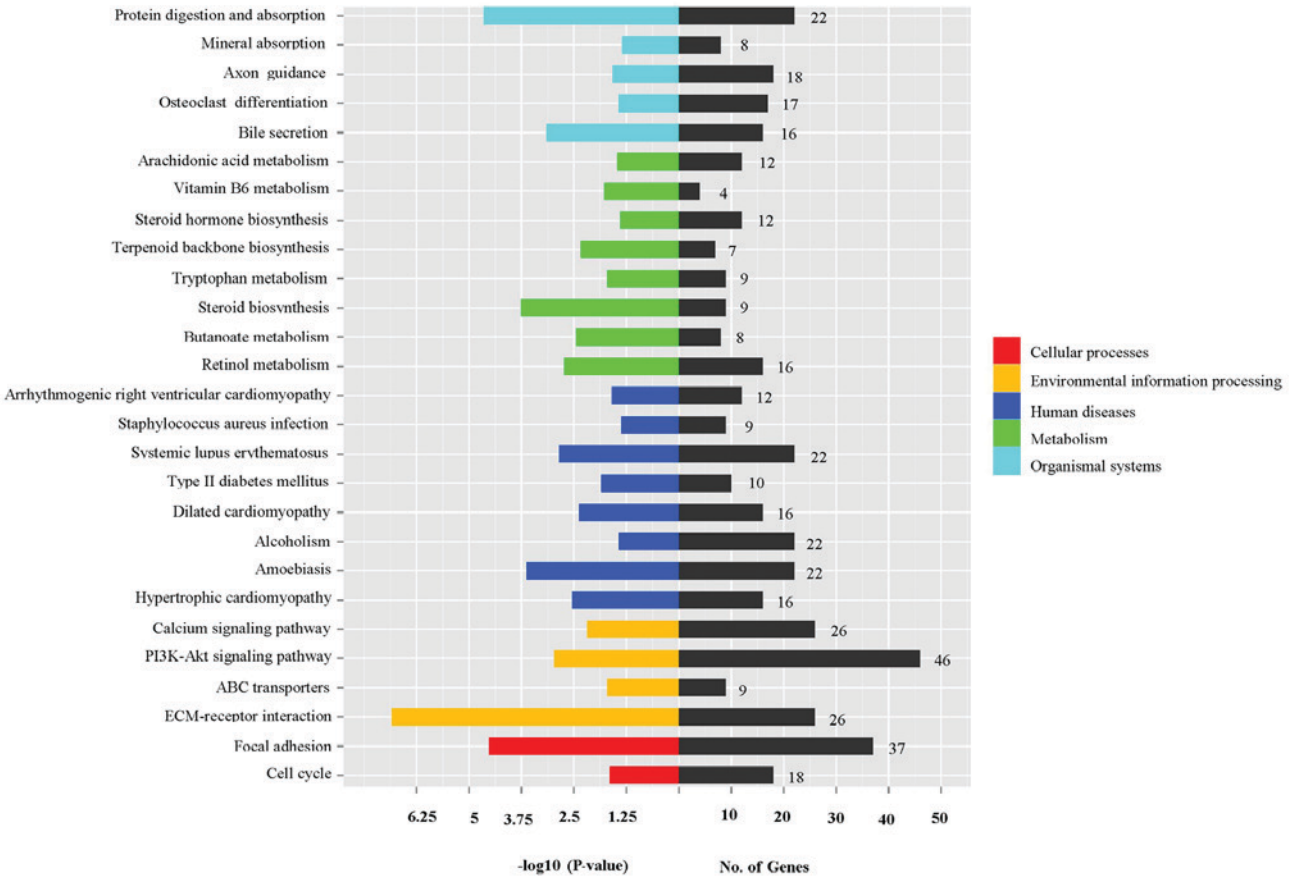

Figure 4. Kyoto Encyclopedia of Genes and Genomes pathway analysis of differentially expressed mRNAs in liver fibrosis.

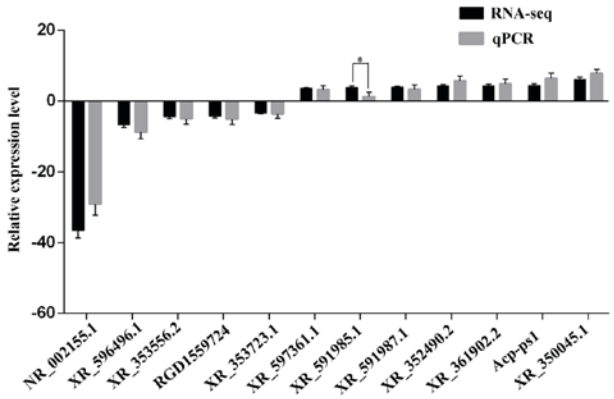

Figure 5. Validation of significantly differentially expressed lncRNAs via RT-qPCR. RT-qPCR results for differentially expressed lncRNAs, with the exception of XR_591985.1, were consistent with those determined by RNA sequencing. RNA sequencing and RT-qPCR data are presented as the mean ± standard deviation. *P<0.05, as indicated. lncRNAs, long noncoding RNAs; RT-qPCR, reverse transcription-quantitative polymerase chain reaction; RNA-seq, RNA sequencing.

genes were predominantly enriched in three pathways, including 'ECM-receptor interaction', 'PI3K-Akt signaling pathway' and 'focal adhesion'.

Validation by RT-qPCR. In order to verify the RNA sequencing data, 12 differentially expressed lncRNAs (nucleotides <5,000; fold-change >3) were chosen for further analysis, 7 of which were upregulated lncRNAs and 5 of which were downregulated lncRNAs. RNA was extracted from all preserved liver tissues and RT-qPCR was performed to validate the expression of selected lncRNAs. The results demonstrated that the expression levels of 11 lncRNAs were in accordance with the RNA sequencing data (Fig. 5); however, the expression level of XR_591985.1 significantly differed from the results of the RNA sequencing data. These results were considered to successfully verify the reliability of the RNA sequencing results.

Overexpression of NR_002155.1 inhibits HSC-T6 cell proliferation. In order to overexpress the novel lncRNA NR_002155.1, its sequence was subcloned into the adenovirus shuttle plasmid vector pAd-EF1a-GFP (Fig. 6A) and its successful overexpression in HSC-T6 cells was confirmed using RT-qPCR (Fig. 6B). Furthermore, the results of the CCK-8 assay demonstrated that increasing the expression of NR_002155.1 significantly decreased the proliferation of HSC-T6 cells at 48 and 72 h time intervals (Fig. 6C), thus confirming that NR_002155.1 may suppress the proliferation of HSCs and may therefore inhibit liver fibrosis induced by CCl_4.

Discussion

CCl_4 administration leads to the infiltration of inflammatory cells and subsequent liver damage leads to the development of fibrosis. In order to investigate the lncRNAs and mRNAs involved in the progression of liver fibrosis, an animal model of liver injury and fibrosis was constructed using male Sprague-Dawley rats treated with CCl_4. The predominant biological processes and pathways enriched in the overlapping differentially expressed mRNAs were revealed. Following this, the differentially expressed lncRNAs were analyzed and their expression levels were verified using RT-qPCR. Finally, one of the most significant differentially expressed lncRNAs, NR_002155.1, was investigated further in order to determine its role in liver fibrosis.

The results of the present study revealed that liver tissues from rats in the CCl_4-treated group exhibited signs of inflammation and the occurrence of fibrosis. The body weight and liver/body weight ratio of the rats were decreased following CCl_4 treatment for 8 weeks. Furthermore, circulating levels of liver function indicators (Alt, Ast, Tgf-β1 and Tnf-α) were significantly enhanced in the CCl_4 treated group. In addition, histological staining indicated that there was marked inflammatory infiltration, collagen deposition and liver fibrosis in the CCl_4-treated liver tissues. Therefore, it may be hypothesized that the aforementioned consequences resulted from the basic toxicity of CCl_4, and this conclusion would be in accordance with the findings of previous studies (23,24).

When liver tissues and cells are exposed to CCl_4, a complex process inducing resistance to toxicity occurs. CCl_4 metabolism in liver tissues or cells induces the generation of free radicals (25) and thus triggers oxidative stress, which results in the initiation and progression of liver damage (26). Furthermore, oxidative stress enhances the secretion of inflammatory cytokines, induces inflammation and necrosis of hepatocytes, and promotes the progression of liver fibrosis (27). These pathological consequences of oxidative stress were demonstrated by the present study, in which levels of Alt, Ast, Tgf-β1 and Tnf-α were increased in the serum of CCl_4-treated rats compared with untreated rats.

GO analysis in the present study revealed that 1,306 mRNAs were differentially expressed in liver tissues from CCl_4-treated rats compared with the untreated group. These differentially expressed mRNAs were predominantly enriched in 'extracellular matrix', 'response to external stimulus', 'cell adhesion' and 'biological adhesion'. With regards to KEGG pathway analysis, the differentially expressed mRNAs in the CCl_4-treated liver tissues were demonstrated to be predominantly enriched in three pathways: 'ECM-receptor interaction', 'PI3K-Akt' and 'focal adhesion'.

HSCs are a type of hepatic nonparenchymal cell, and their activation and proliferation are involved in liver fibrosis. HSCs exposed to chronic injury are activated and undergo proliferation. Excessive proliferation of HSCs leads to the secretion of excessive levels of ECM, thus causing abnormal ECM deposition. Abundant ECM has the potential to replace normal hepatocytes (28), which contributes to scar formation and fibrosis (29). These previous findings were verified in the present study via Masson staining. ECM-receptor interaction, associated with signaling pathways involved in paracrine/endocrine functioning, may affect cell phenotype, adhesion, migration, proliferation and differentiation (30). The focal adhesion signaling pathway primarily involves integrin and focal adhesion kinase (FAK). As a tyrosine kinase receptor, FAK is reported to be activated by platelet-derived growth factor (PDGF) and, following interaction with ECM proteins via association with integrin, FAK directly senses the integrity of the extracellular environment (31-33). The activation of FAK has been reported to be essential for PDGF-induced HSC proliferation (34). As a key downstream kinase of integrin/FAK, phosphoinositide 3-kinase (PI3K) is also activated

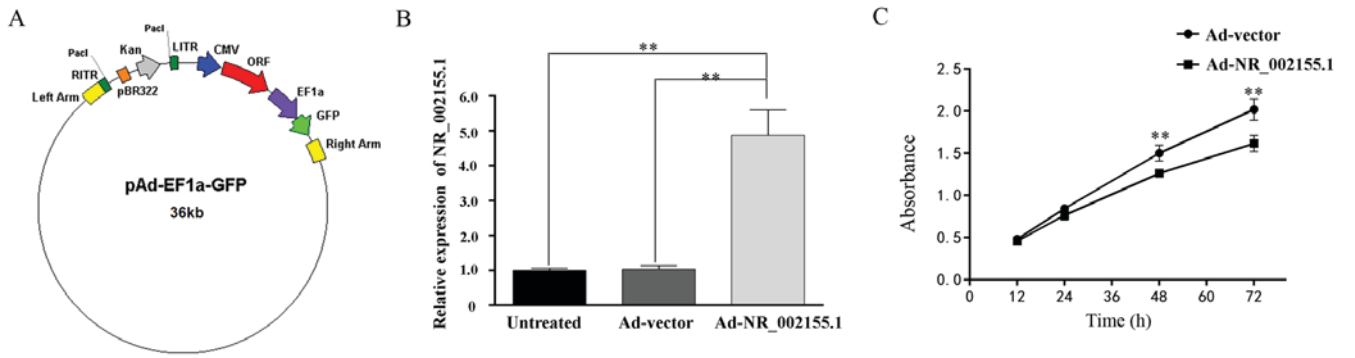

Figure 6. Effects of overexpression of NR_002155.1 on HSC proliferation. (A) Schematic of the adenovirus shuttle plasmid vector pAd-EF1a-GFP. (B) Expression of NR_002155.1 was significantly enhanced in the Ad-NR_002155.1 group compared with the Ad-vector and untreated groups. (C) HSC proliferation was significantly suppressed following overexpression of NR_002155.1. For part B, $^{**}P<0.01$, as indicated; for part C, $^{**}P<0.01$ vs. Ad-NR_002155.1 group. HSCs, hepatic stellate cells.

by PDGF stimulation and response to the proliferation of PDGF-induced HSCs (34,35). Stimulation of the PI3K pathway has been demonstrated to be essential for HSC proliferation *in vitro* and in CCl_4-induced rat liver fibrosis *in vivo* (36). Akt, which is positioned downstream of PI3K, is also reported to be involved in the stimulation of cell proliferation and inhibition of cell apoptosis in HSCs (37,38). Type I collagen gene expression was demonstrated to be primarily regulated by the PI3K-Akt pathway (34). The expression levels of type I collagen mRNA and protein were significantly reduced by the PI3K inhibitor LY294002 or by inhibition of Akt expression via adenoviral-mediated transduction with a dominant negative form of Akt (39). Therefore, the ECM-receptor interaction, focal adhesion and the PI3K-Akt pathways all interact with each other in order to regulate the process of fibrogenesis.

In the present study, RNA sequencing demonstrated that 231 lncRNAs were significantly differentially expressed (fold-change >2) between CCl_4-treated and untreated rats' liver tissue. The majority of identified lncRNAs were not previously reported and the functions of these lncRNAs remain unknown. RT-qPCR analyses were performed to verify the reliability of the RNA sequencing data. The expression levels of the selected lncRNAs determined by RT-qPCR were consistent with RNA sequencing data. In order to verify whether the differentially expressed lncRNAs identified by RNA sequencing contribute to the progression of liver fibrosis, the biological function of NR_002155.1 was investigated (fold-change=36.6). NR_002155.1, a newly identified long noncoding RNA with a length of 951 base pairs, to the best of our knowledge, has not been previously investigated. In the present study, it was demonstrated that NR_002155.1 may inhibit HSC-T6 cell proliferation *in vitro*, which is consistent with the findings of the RNA sequencing analysis.

In conclusion, the expression profile of lncRNAs in CCl_4-induced liver fibrosis was determined via RNA sequencing and differentially expressed lncRNAs and mRNAs were identified. Differentially expressed mRNAs between liver tissues from CCl_4-treated and untreated rats were predominantly enriched in the 'ECM-receptor interaction', 'focal adhesion' and 'PI3K-Akt signaling pathway' path ways. Following validation of these results by RT-qPCR analysis, the biological function of the aberrantly expressed lncRNA NR_002155.1 was investigated. The results of the *in vitro* function experiments indicated that lncRNA NR_002155.1 may inhibit the proliferation of HSCs *in vitro* and *in vivo*. However, the mechanisms of the identified lncRNAs in liver fibrosis are yet to be determined. Future studies should further investigate the association and network construction between the lncRNAs and mRNAs identified in the present study. In addition, further studies should explore the biological functions and regulatory mechanisms of lncRNAs, which may uncover novel diagnostic biomarkers and effective therapeutic strategies for liver fibrosis.

Acknowledgements

Not applicable.

Funding

The present study was supported by the National Natural Science Foundation of China (grant no. 81473473), the Education Department of Jiangxi Province (grant no. GJJ160039), the Science Technology and Innovation Commission of Shenzhen Municipality in China (grant no. JCYJ20160428173252471) and the Health and Family Planning Commission of Shenzhen Municipality in China (grant no. SZSM201512026).

Availability of data and materials

All data generated or analyzed during this study are included in this published article.

Authors' contributions

ZG, JT, TX, JL and CD performed the experiments. ZG, YP, JZ and GH analyzed and interpreted the RNA sequencing data. ZG and GH were major contributors in writing the manuscript. All authors read and approved the final manuscript.

Ethics approval and consent to participate

Animal experiments were approved by the Animal Ethics Committee of Peking University Shenzhen Hospital (Shenzhen, China).

Consent for publication

Not applicable.

Competing interests

The authors declare that they have no competing interests.

References

1. Duval F, Moreno-Cuevas JE, Gonzalez-Garza MT, Maldonado-Bernal C and Cruz-Vega DE: Liver fibrosis and mechanisms of the protective action of medicinal plants targeting inflammation and the immune response. Int J Inflam 2015: 943497, 2015.
2. Enomoto M, Morikawa H, Tamori A and Kawada N: Noninvasive assessment of liver fibrosis in patients with chronic hepatitis B. World J Gastroenterol 20: 12031-12038, 2014.
3. Xuan J, Chen S, Ning B, Tolleson WH and Guo L: Development of HepG2-derived cells expressing cytochrome P450s for assessing metabolism-associated drug-induced liver toxicity. Chem Biol Interact 255: 63-73, 2016.
4. Huang ZG, Zhai WR, Zhang YE and Zhang XR: Study of heteroserum-induced rat liver fibrosis model and its mechanism. World J Gastroenterol 4: 206-209, 1998.
5. Novikova IV, Hennelly SP and Sanbonmatsu KY: Sizing up long non-coding RNAs: Do lncRNAs have secondary and tertiary structure? Bioarchitecture 2: 189-199, 2012.
6. Geisler S and Coller J: RNA in unexpected places: Long non-coding RNA functions in diverse cellular contexts. Nat Rev Mol Cell Biol 14: 699-712, 2013.
7. Gibb EA, Brown CJ and Lam WL: The functional role of long non-coding RNA in human carcinomas. Mol Cancer 10: 38, 2011.
8. Li J, Tian H, Yang J and Gong Z: Long noncoding RNAs regulate cell growth, proliferation, and apoptosis. DNA Cell Biol 35: 459-470, 2016.
9. Briggs JA, Wolvetang EJ, Mattick JS, Rinn JL and Barry G: Mechanisms of long Non-coding RNAs in mammalian nervous system development, plasticity, disease, and evolution. Neuron 88: 861-877, 2015.
10. Schmitt AM and Chang HY: Long noncoding RNAs in cancer pathways. Cancer Cell 29: 452-463, 2016.
11. Roberts TC, Morris KV and Weinberg MS: Perspectives on the mechanism of transcriptional regulation by long non-coding RNAs. Epigenetics 9: 13-20, 2014.
12. Wang KC and Chang HY: Molecular mechanisms of long noncoding RNAs. Mol Cell 43: 904-914, 2011.
13. Yu F, Zheng J, Mao Y, Dong P, Li G, Lu Z, Guo C, Liu Z and Fan X: Long non-coding RNA APTR promotes the activation of hepatic stellate cells and the progression of liver fibrosis. Biochem Biophys Res Commun 463: 679-685, 2015.
14. Wu Y, Liu X, Zhou Q, Huang C, Meng X, Xu F and Li J: Silent information regulator 1 (SIRT1) ameliorates liver fibrosis via promoting activated stellate cell apoptosis and reversion. Toxicol Appl Pharmacol 289: 163-176, 2015.
15. He Y, Wu YT, Huang C, Meng XM, Ma TT, Wu BM, Xu FY, Zhang L, Lv XW and Li J: Inhibitory effects of long noncoding RNA MEG3 on hepatic stellate cells activation and liver fibrogenesis. Biochim Biophys Acta 1842: 2204-2215, 2014.
16. Yu F, Zheng J, Mao Y, Dong P, Lu Z, Li G, Guo C, Liu Z and Fan X: Long Non-coding RNA growth Arrest-specific transcript 5 (GAS5) inhibits liver fibrogenesis through a mechanism of competing endogenous RNA. J Biol Chem 290: 28286-28298, 2015.
17. Kong X, Zhou W, Wan JB, Zhang Q, Ni J and Hu Y: An integrative thrombosis network: Visualization and topological analysis. Evid Based Complement Alternat Med 2015: 265303, 2015.
18. National Research Council: Guide for the Care and Use of Laboratory Animals. The National Academies Press, Washington, DC, 1996. https://www.nap.edu/catalog/5140/guide-for-the-care-and-use-of-laboratory-animals.
19. Livak KJ and Schmittgen TD: Analysis of relative gene expression data using real-time quantitative PCR and the 2(-Delta Delta C(T)) method. Methods 25: 402-408, 2001.
20. Trapnell C, Pachter L and Salzberg SL: TopHat: Discovering splice junctions with RNA-Seq. Bioinformatics 25: 1105-1111, 2009.
21. Feng J, Meyer CA, Wang Q, Liu JS, Shirley Liu X and Zhang Y: GFOLD: A generalized fold-change for ranking differentially expressed genes from RNA-seq data. Bioinformatics 28: 2782-2788, 2012.
22. Trapnell C, Roberts A, Goff L, Pertea G, Kim D, Kelley DR, Pimentel H, Salzberg SL, Rinn JL and Pachter L: Differential gene and transcript expression analysis of RNA-seq experiments with TopHat and Cufflinks. Nat Protoc 7: 562-578, 2012.
23. Dong S, Chen QL, Song YN, Sun Y, Wei B, Li XY, Hu YY, Liu P and Su SB: Mechanisms of CCl4-induced liver fibrosis with combined transcriptomic and proteomic analysis. J Toxicol Sci 41: 561-572, 2016.
24. Marques TG, Chaib E, da Fonseca JH, Lourenço AC, Silva FD, Ribeiro MA Jr, Galvão FH and D'Albuquerque LA: Review of experimental models for inducing hepatic cirrhosis by bile duct ligation and carbon tetrachloride injection. Acta Cir Bras 27: 589-594, 2012.
25. Sancheti S, Sancheti S and Seo SY: Ameliorative effects of 7-methylcoumarin and 7-methoxycoumarin against CCl4-induced hepatotoxicity in rats. Drug Chem Toxicol 36: 42-47, 2013.
26. Li S, Tan HY, Wang N, Zhang ZJ, Lao L, Wong CW and Feng Y: The role of oxidative stress and antioxidants in liver diseases. Int J Mol Sci 16: 26087-26124, 2015.
27. Heeba GH and Mahmoud ME: Therapeutic potential of morin against liver fibrosis in rats: Modulation of oxidative stress, cytokine production and nuclear factor kappa B. Environ Toxicol Pharmacol 37: 662-671, 2014.
28. Duval F, Moreno-Cuevas JE, Gonzalez-Garza MT, Rodriguez-Montalvo C and Cruz-Vega DE: Protective mechanisms of medicinal plants targeting hepatic stellate cell activation and extracellular matrix deposition in liver fibrosis. Chin Med 9: 27, 2014.
29. Roy S, Benz F, Vargas Cardenas D, Vucur M, Gautheron J, Schneider A, Hellerbrand C, Pottier N, Alder J, Tacke F, *et al*: miR-30c and miR-193 are a part of the TGF-β-dependent regulatory network controlling extracellular matrix genes in liver fibrosis. J Dig Dis 16: 513-524, 2015.
30. Karsdal MA, Manon-Jensen T, Genovese F, Kristensen JH, Nielsen MJ, Sand JM, Hansen NU, Bay-Jensen AC, Bager CL, Krag A, *et al*: Novel insights into the function and dynamics of extracellular matrix in liver fibrosis. Am J Physiol Gastrointest Liver Physiol 308: G807-G830, 2015.
31. Carloni V, Romanelli RG, Pinzani M, Laffi G and Gentilini P: Focal adhesion kinase and phospholipase C gamma involvement in adhesion and migration of human hepatic stellate cells. Gastroenterology 112: 522-531, 1997.
32. Renshaw MW, Price LS and Schwartz MA: Focal adhesion kinase mediates the integrin signaling requirement for growth factor activation of MAP kinase. J Cell Biol 147: 611-618, 1999.
33. Wang Y, Ma J, Chen L, Xie XL and Jiang H: Inhibition of focal adhesion kinase on hepatic Stellate-cell adhesion and migration. Am J Med Sci 353: 41-48, 2017.
34. Reif S, Lang A, Lindquist JN, Yata Y, Gabele E, Scanga A, Brenner DA and Rippe RA: The role of focal adhesion kinase-phosphatidylinositol 3-kinase-akt signaling in hepatic stellate cell proliferation and type I collagen expression. J Biol Chem 278: 8083-8090, 2003.
35. Novo E, Cannito S, Paternostro C, Bocca C, Miglietta A and Parola M: Cellular and molecular mechanisms in liver fibrogenesis. Arch Biochem Biophys 548: 20-37, 2014.
36. Lin X, Bai F, Nie J, Lu S, Lu C, Zhu X, Wei J, Lu Z and Huang Q: Didymin alleviates hepatic fibrosis through inhibiting ERK and PI3K/Akt pathways via regulation of raf kinase inhibitor protein. Cell Physiol Biochem 40: 1422-1432, 2016.
37. Kim AH, Khursigara G, Sun X, Franke TF and Chao MV: Akt phosphorylates and negatively regulates apoptosis signal-regulating kinase 1. Mol Cell Biol 21: 893-901, 2001.
38. Coffer PJ, Jin J and Woodgett JR: Protein kinase B (c-Akt): A multifunctional mediator of phosphatidylinositol 3-kinase activation. Biochem J 335: 1-13, 1998.
39. Ricupero DA, Poliks CF, Rishikof DC, Cuttle KA, Kuang PP and Goldstein RH: Phosphatidylinositol 3-kinase-dependent stabilization of alpha1(I) collagen mRNA in human lung fibroblasts. Am J Physiol Cell Physiol 281: C99-C105, 2001.